

## Scintillation Properties of Eu:CaS Transparent Ceramics for Radiation Imaging Applications

Hiromi Kimura,<sup>1\*</sup> Takeshi Fujiwara,<sup>1</sup> Hidetoshi Kato,<sup>1</sup> Takumi Kato,<sup>2</sup> Toshiaki Kunikata,<sup>2</sup> Noriaki Kawaguchi,<sup>2</sup> and Takayuki Yanagida<sup>2</sup>

<sup>1</sup>National Institute of Advanced Industrial Science and Technology (AIST),  
1-1-1 Umezono, Tsukuba, Ibaraki 305-8568, Japan

<sup>2</sup>Division of Materials Science, Nara Institute of Science and Technology (NAIST),  
8916-5 Takayama, Ikoma, Nara 630-0192, Japan

(Received October 31, 2025; accepted December 12, 2025)

**Keywords:** radiation-induced luminescence, scintillators, X-ray imaging detectors

CaS transparent ceramics doped with various concentrations of Eu (0.01, 0.05, 0.1, and 0.5%) were synthesized by the spark plasma sintering method, and their structural, optical, and X-ray-induced scintillation properties were evaluated. The ceramics exhibited high transmittance (~80%) with absorption bands corresponding to the 4f–5d transitions of Eu<sup>2+</sup> ions at 300–350 nm and 400–600 nm. Under UV and X-ray excitation, a broad emission peak at around 650 nm was observed, which would be due to the 5d–4f transitions of Eu<sup>2+</sup> ions. The practical applicability of the 0.05% Eu-doped CaS transparent ceramic was demonstrated through X-ray imaging of electronic components. The X-ray imaging system achieved a spatial resolution of at least 0.15 mm.

### 1. Introduction

X-ray imaging has been applied in a wide range of fields, including medical diagnostics,<sup>(1,2)</sup> security,<sup>(3,4)</sup> and industrial inspection.<sup>(5–8)</sup> Among the detectors used in these applications, scintillation detectors are widely used and typically consist of a combination of a scintillator and a photodetector. Scintillators convert the energy of absorbed ionizing radiation into numerous low-energy photons, which are subsequently converted into electrons by photodetectors such as photomultiplier tubes or Si-photodiodes. Scintillators for X-ray detectors are required to have high light yield, low afterglow, and high detection efficiency. Since the required properties depend on the application, various types of scintillator have been developed.<sup>(9–13)</sup>

To date, most scintillators have been used in the bulk single crystal form, owing to their high optical quality. Recently, transparent ceramics have attracted significant attention for radiation detection applications.<sup>(14–22)</sup> Previous studies have shown that transparent ceramic materials such as Ce-doped Gd<sub>3</sub>Al<sub>2</sub>Ga<sub>3</sub>O<sub>12</sub>,<sup>(23)</sup> Ce-doped Lu<sub>3</sub>Al<sub>5</sub>O<sub>12</sub>,<sup>(24)</sup> Eu-doped BaFCl,<sup>(25)</sup> and Eu-doped SrCl<sub>2</sub><sup>(26)</sup> can exhibit scintillation performance surpassing that of single crystals with

\*Corresponding author: e-mail: [h.kimura@aist.go.jp](mailto:h.kimura@aist.go.jp)  
<https://doi.org/10.18494/SAM6031>

identical chemical compositions. In this work, we focus on sulfide transparent ceramics because sulfide scintillators such as ZnS:Ag and Lu<sub>2</sub>S<sub>3</sub>:Ce have been reported to exhibit high scintillation intensity.<sup>(27,28)</sup> As the new sulfide scintillators, Eu-doped CaS powders have also attracted attention as a phosphor material, and in previous studies, its use in X-ray detection has been explored.<sup>(29,30)</sup> However, research has been limited to opaque ceramic forms because sulfide single crystals are difficult to grow from the melt owing to the easy formation of sulfur vacancies.<sup>(26,31)</sup> Therefore, we have developed Eu-doped CaS transparent ceramics formed by the spark plasma sintering (SPS) technique and investigated their structural, optical, and X-ray-induced scintillation properties.

## 2. Experimental Methods

Eu-doped CaS transparent ceramics were synthesized by the SPS technique. As starting materials, the raw powders of EuS (Kojundo Chemical Lab., Purity: 99.9%) and CaS (Kojundo Chemical Lab., Purity: 99.99%) were used and uniformly mixed. The mixture was then placed into a graphite die and compressed between two graphite punches. The internal surface was covered with a graphite sheet of 0.2 mm thickness. Sintering was performed using an SPS furnace (Sinter Land, LABOX-215GH). During sintering, the temperature was raised to 1700 °C at a heating rate of 10 °C/min and maintained for 1 h under a vacuum atmosphere (~10 Pa) while a uniaxial pressure of 80 MPa was simultaneously applied. The sintered ceramics were sectioned and the surfaces subsequently polished using sandpaper (600–3000 grits).

To identify the crystalline phase, X-ray diffraction (XRD) patterns were measured with a diffractometer (Rigaku, MiniFlex600). For optical properties, the diffuse transmittance spectra and photoluminescence (PL) excitation/emission maps were obtained using a spectrometer (Shimadzu, SolidSpec-3700) and a Quantaurus-QY spectrometer (Hamamatsu Photonics, C11347), respectively. The X-ray-induced scintillation spectra and afterglow curves were measured using our original systems.<sup>(23,32)</sup> To evaluate the potential for X-ray imaging applications, X-ray imaging was performed using a Peltier-cooled CCD camera (Bitran, CS-66UV) equipped with a lens (PF10545MF-UV, Nikon). During imaging, X-rays were irradiated using an X-ray generator (RXG-0118Mo, R-Tech) operated at 50 kV and 1 mA. As the imaging object, the electric component (24LC64-I/SN, Microchip Technology) with 0.15 mm lead widths within an epoxy resin matrix was used. The object was placed 5 cm from the X-ray target, and the dose rate was 300 mGy/s. X-ray imaging was performed by exposing the samples to X-rays for a duration of 5 s.

## 3. Results and Discussion

XRD patterns of Eu-doped CaS transparent ceramics and the standard card of CaS (COD: 9008606) are described in Fig. 1. All diffraction patterns were consistent with reference data for the face-centered cubic structure of CaS. With increasing Eu concentration, the diffraction peaks gradually shifted toward lower angles. This shift can be attributed to the substitution of Ca<sup>2+</sup> ions (ionic radius: 1.12 Å for coordination number 8) by Eu<sup>2+</sup> ions (ionic radius: 1.25 Å for

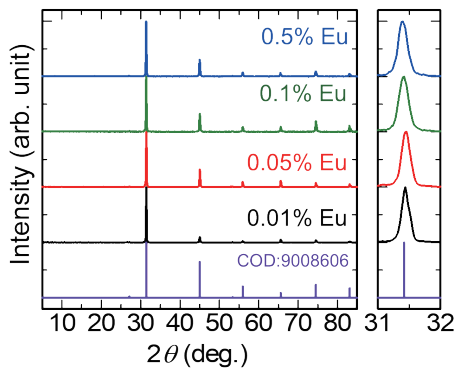


Fig. 1. (Color online) XRD patterns of Eu-doped CaS transparent ceramics and the standard card of CaS (COD: 9008606).

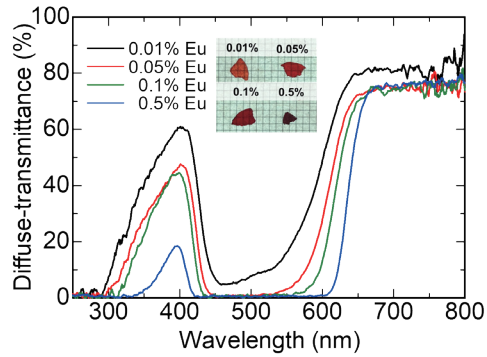


Fig. 2. (Color online) Diffuse-transmittance spectra of Eu-doped CaS transparent ceramics. The inset shows photographs of Eu-doped CaS transparent ceramics.

coordination number 8). Figure 2 shows the diffuse-transmittance spectra and photographs of Eu-doped CaS. In all the ceramics, the mesh patterns behind the ceramics are visible through the ceramics. The ceramics exhibit a red coloration, which became more pronounced with increasing Eu concentration. For the diffuse transmittance spectra, all the ceramics exhibited high transmittance of approximately 80% in the wavelength range of 600–800 nm. A decrease in transmittance at around 300–350 nm and 400–600 nm was observed and was enhanced as the Eu concentration increased. This behavior is attributed to absorption associated with the 4f–5d transitions of Eu<sup>2+</sup> ions.<sup>(33–35)</sup>

Figure 3 shows PL excitation/emission maps of 0.1% Eu-doped CaS transparent ceramic as a representative. Under excitation of around 300–350 nm and 400–600 nm, the broad emission band was observed at around 650 nm, and the spectral shapes of all the ceramics were similar. Since the features of excitation and emission bands were consistent with those reported for Eu-doped CaS opaque ceramics, the emission origin would be the 5d–4f transitions of Eu<sup>2+</sup> ions.<sup>(29,36–39)</sup> The quantum yields of 0.01, 0.05, 0.1, and 0.5% Eu-doped CaS were determined using an integrating sphere under 460 nm excitation, and the obtained values were 16.1, 14.1, 10.1, and 3.2%, respectively. These values are lower than the ~62.7% reported for previously studied Eu-doped CaS opaque ceramics.<sup>(29)</sup> In earlier studies, EuCl<sub>3</sub> was used as the dopant, whereas in the present work, EuS was employed. In addition, the sintering temperature used in this study (1700 °C) was higher than that reported previously (1000 °C). These differences in the starting materials and sintering conditions may have affected the quantum yields.

X-ray-induced scintillation spectra of Eu-doped CaS transparent ceramics are shown in Fig. 4. The shapes of the scintillation spectra were similar to those of the PL spectra, and the emission at around 650 nm matches the wavelength sensitivity of the Si-photodiode. With increasing Eu concentration, the emission peak positions shifted toward longer wavelengths. This wavelength shift is attributed to self-absorptions of Eu<sup>2+</sup> ions, as indicated by the diffuse-transmittance spectra shown in Fig. 2. The inset of Fig. 4 shows the integrated scintillation intensity of Eu-doped CaS transparent ceramics. In general, the integrated scintillation intensity depends on the output signal when used with integrating detectors, such as X-ray imaging systems. Among all

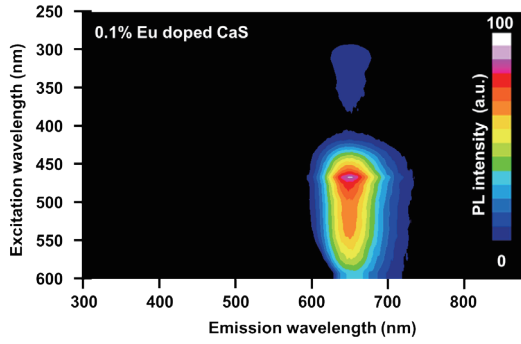


Fig. 3. (Color online) PL excitation/emission maps and QY values of the Eu-doped CaS transparent ceramics.

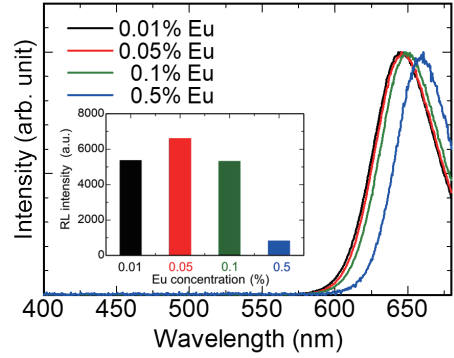


Fig. 4. (Color online) X-ray-induced scintillation spectra of Eu-doped CaS transparent ceramics. The inset shows the integrated scintillation intensity of Eu-doped CaS transparent ceramics.

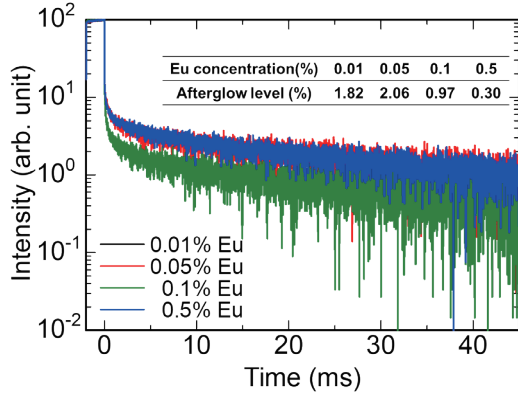


Fig. 5. (Color online) Afterglow curves of Eu-doped CaS transparent ceramics with 2 ms X-ray irradiation. The inset summarizes the afterglow levels.

the ceramics, 0.05% Eu-doped CaS exhibited the highest emission intensity, suggesting that the optimal Eu doping concentration in CaS transparent ceramics is approximately 0.05%.

Afterglow curves of Eu-doped CaS transparent ceramics with 2 ms X-ray irradiation are shown in Fig. 5. Here, the afterglow levels were calculated using the following equation:  $(I_2 - I_{BG})/(I_1 - I_{BG})$ , where  $I_1$  is the intensity during X-ray irradiation,  $I_2$  is the intensity at 20 ms after X-ray cut off, and  $I_{BG}$  is the background intensity. The calculated afterglow levels are summarized in the inset of Fig. 5. Compared with the commercially available Tl:CsI scintillator, which has an afterglow level of  $\sim 0.04\%$ ,<sup>(40,41)</sup> the Eu-doped CaS transparent ceramics exhibited afterglow levels one to two orders of magnitude higher. If the near-room-temperature trap levels that cause afterglow can be reduced by introducing codopants or optimizing the sintering conditions, further improvement in the afterglow properties can be expected.<sup>(42,43)</sup>

Figure 6 shows the real-time X-ray imaging system and an X-ray image of an electric component using a 0.05% Eu-doped CaS transparent ceramic. The electric component, which

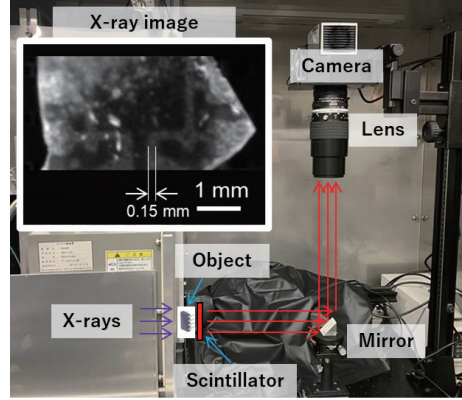


Fig. 6. (Color online) Schematic of the real-time X-ray imaging system and an X-ray image of an electric component using a 0.05% Eu-doped CaS transparent ceramic.

contains 0.15 mm lead widths within an epoxy resin matrix, was imaged to demonstrate that the X-ray imaging system employing 0.05% Eu-doped CaS transparent ceramics can achieve a spatial resolution of at least 0.15 mm. While this imaging test is preliminary, optimizing the scintillator thickness and detector setup may lead to higher spatial resolution. Consequently, the 0.05% Eu-doped CaS transparent ceramic shows potential as a scintillator for X-ray imaging applications.

#### 4. Conclusions

We synthesized 0.01–0.5% Eu-doped CaS transparent ceramics by the SPS method, and their structural, optical, and X-ray-induced scintillation properties were investigated. All the ceramics exhibited high transmittance (~80%), and the absorption bands due to 4f–5d transitions of Eu<sup>2+</sup> were confirmed at around 300–350 and 400–600 nm. Under UV excitation (300–350 and 400–600 nm) and X-ray irradiation, the broad emission band at around 650 nm was observed, which was suitable for the wavelength sensitivity of the Si-photodiode. The X-ray imaging test was performed using 0.05% Eu-doped CaS, confirming that the spatial resolution was at least 0.15 mm. The Eu-doped CaS transparent ceramic was regarded as a promising candidate scintillator for X-ray imaging applications.

#### Acknowledgments

This work was supported by ACT-X (JPMJAX23K8) from JST and Grants-in-Aid for Early-Career Scientists (25K21506) and Young Scientists (24KJ1693) from the Japan Society for the Promotion of Science.

#### References

- 1 M. J. Yaffe and J. A. Rowlands: *Phys. Med. Biol.* **42** (1997) 1.
- 2 C. W. E. van Eijk: *Phys. Med. Biol.* **47** (2002) R85.
- 3 A. Mohanarathinam, S. Kamalraj, G. K. D. Prasanna Venkatesan, R. V. Ravi, and C. S. Manikandababu: *J. Ambient Intell. Humaniz. Comput.* **11** (2020) 3221.
- 4 K. Wells and D. A. Bradley: *Appl. Radiat. Isot.* **70** (2012) 1729.
- 5 C. Connolly: *Sens. Rev.* **28** (2008) 194.
- 6 H. Kimura, H. Fukushima, K. Watanabe, T. Fujiwara, H. Kato, M. Tanaka, T. Kato, D. Nakauchi, N. Kawaguchi, and T. Yanagida: *Sens. Mater.* **36** (2024) 507.
- 7 T. Fujiwara, H. Miyoshi, Y. Mitsuya, N. L. Yamada, Y. Wakabayashi, Y. Otake, M. Hino, K. Kino, M. Tanaka, N. Oshima, and H. Takahashi: *Rev. Sci. Instrum.* **93** (2022).
- 8 T. Fujiwara, S. Tanaka, Y. Mitsuya, H. Takahashi, K. Tagi, J. Kusano, E. Tanabe, M. Yamamoto, N. Nakamura, K. Dobashi, H. Tomita, and M. Uesaka: *J. Instrum.* **8** (2013) C12020.
- 9 C. Greskovich and S. Duclos: *Annu. Rev. Mater. Sci.* **27** (1997) 69.
- 10 T. Kunikata, K. Okazaki, H. Kimura, S. Takase, T. Kato, D. Nakauchi, N. Kawaguchi, and T. Yanagida: *Sens. Mater.* **37** (2025) 563.
- 11 M. Ishida, A. Watanabe, H. Kawamoto, Y. Fujimoto, and K. Asai: *Sens. Mater.* **37** (2025) 607.
- 12 T. Yanagida, T. Kato, D. Nakauchi, and N. Kawaguchi: *Jpn. J. Appl. Phys.* **62** (2023) 010508.
- 13 M. Koshimizu: *Jpn. J. Appl. Phys.* **62** (2023) 010503.
- 14 S. Otake, S. Takase, T. Kato, D. Nakauchi, N. Kawaguchi, and T. Yanagida: *Sens. Mater.* **37** (2025) 519.
- 15 S. Otake, H. Sakaguchi, Y. Yoshikawa, T. Kato, D. Nakauchi, N. Kawaguchi, and T. Yanagida: *Sens. Mater.* **36** (2024) 539.

- 16 H. Kimura, T. Kato, T. Fujiwara, M. Tanaka, D. Nakauchi, N. Kawaguchi, and T. Yanagida: *Jpn. J. Appl. Phys.* **62** (2023) 010504.
- 17 T. Wang, S. Hu, T. Ji, X. Zhu, G. Zeng, L. Huang, A. N. Yakovlev, J. Qiu, X. Xu, and X. Yu: *Laser Photon. Rev.* **18** (2024) 2300892.
- 18 D. Shiratori, H. Kimura, Y. Fukuchi, and T. Yanagida: *Sens. Mater.* **36** (2024) 547.
- 19 A. Volfi, L. Esposito, V. Biasini, A. Piancastelli, and J. Hostaša: *Open Ceram.* **20** (2024) 100682.
- 20 A. M. Tsabit and D.-H. Yoon: *J. Korean Ceram. Soc.* **59** (2022) 1.
- 21 H. Kimura, T. Kato, T. Fujiwara, M. Tanaka, G. Okada, D. Nakauchi, N. Kawaguchi, and T. Yanagida: *Ceram. Int.* **49** (2023) 15315.
- 22 T. Kato, D. Nakauchi, N. Kawaguchi, and T. Yanagida: *Sens. Mater.* **36** (2024) 531.
- 23 T. Yanagida, K. Kamada, Y. Fujimoto, H. Yagi, and T. Yanagitani: *Opt. Mater.* **35** (2013) 2480.
- 24 T. Yanagida, Y. Fujimoto, Y. Yokota, K. Kamada, S. Yanagida, A. Yoshikawa, H. Yagi, and T. Yanagitani: *Radiat. Meas.* **46** (2011) 1503.
- 25 S. Otake, T. Kato, D. Nakauchi, N. Kawaguchi, and T. Yanagida: *J. Lumin.* **275** (2024) 120828.
- 26 T. Ubukata, S. Otake, T. Kato, D. Nakauchi, N. Kawaguchi, and T. Yanagida: *J. Lumin.* **278** (2025) 121021.
- 27 R. H. Hughes: *Rev. Sci. Instrum.* **31** (1960) 1156.
- 28 J. C. van't Spijker, P. Dorenbos, C. P. Allier, C. W. E. van Eijk, A. R. H. F. Ettema, and G. Huber: *Nucl. Instruments Methods Phys. Res. Sect. B Beam Interact. with Mater. Atoms* **134** (1998) 304.
- 29 M. Arai, Y. Fujimoto, M. Koshimizu, I. Kawamura, D. Nakauchi, T. Yanagida, and K. Asai: *J. Ceram. Soc. Japan* **128** (2020) 523.
- 30 H. Nanto and G. Okada: *Phosphors Radiat. Detect.* (Wiley, 2022) pp. 225–245.
- 31 K. Realo, A. Maaroos, A. Haav, and I. Jaek: *J. Cryst. Growth* **56** (1982) 639.
- 32 T. Yanagida, Y. Fujimoto, T. Ito, K. Uchiyama, and K. Mori: *Appl. Phys. Express* **7** (2014) 062401.
- 33 A. Cho, S. Y. Kim, M. Lee, S.-J. Kim, C.-H. Kim, and C.-H. Pyun: *J. Lumin.* **91** (2000) 215.
- 34 D. Jia, W. Jia, D. R. Evans, W. M. Dennis, H. Liu, J. Zhu, and W. M. Yen: *J. Appl. Phys.* **88** (2000) 3402.
- 35 H. Zhi-yi, W. Yong-sheng, S. Li, and X. Xu-rong: *J. Phys. Condens. Matter* **13** (2001) 3665.
- 36 W. Lehmann and F. M. Ryan: *J. Electrochem. Soc.* **118** (1971) 477.
- 37 S. Kijima, K. Sato, and T. Koda: *J. Lumin.* **55** (1993) 187.
- 38 N. Yamashita, S. Fukumoto, S. Ibuki, and H. Ohnishi: *Jpn. J. Appl. Phys.* **32** (1993) 3135.
- 39 K. N. Kim, J. Kim, K. J. Choi, J. K. Park, and C. H. Kim: *J. Am. Ceram. Soc.* **89** (2006) 3413.
- 40 K. Takahashi, H. Kimura, D. Nakauchi, T. Kato, N. Kawaguchi, and T. Yanagida: *Jpn. J. Appl. Phys.* **59** (2020) 122005.
- 41 H. Kimura, T. Fujiwara, R. Suzuki, and H. Kato: *J. Lumin.* **287** (2025) 121485.
- 42 D. Totsuka, T. Yanagida, Y. Fujimoto, Y. Yokota, F. Moretti, A. Vedda, and A. Yoshikawa: *Appl. Phys. Express* **5** (2012) 052601.
- 43 D. Jia, W. Jia, D. R. Evans, W. M. Dennis, H. Liu, J. Zhu, and W. M. Yen: *J. Appl. Phys.* **88** (2000) 3402.